

Supporting Information

**Covalent organic framework-MnO₂ nanoparticle
composites for shape selective sensing of biothiols**

Yuping Cao^{a,1}, Jin Zhang^{a,1}, Jilu Yang^a, Wenwu Qin^{a*}

^aKey Laboratory of Nonferrous Metal Chemistry and Resources Utilization of Gansu Province, State Key Laboratory of Applied Organic Chemistry, Key Laboratory of Special Function Materials and Structure Design (MOE), and College of Chemistry and Chemical Engineering, Lanzhou University, Lanzhou 730000, P. R. China

* Corresponding author: Fax: +86-931-8912582 E-mail address: qinww@lzu.edu.cn
(W. Qin)

¹ These authors contributed equally to this article.

Synthesis of 2,5-dimethoxybenzene-1,4- dicarboxaldehyde (Dp) :

1,4-dibromo-2,5-dimethoxybenzene (1g, 3.4mmol) was added to 40mL of dry THF at -78° C under N₂ atmosphere. The mixture was stirring in -78°C until 1,4-dibromo-2,5-dimethoxybenzene dissolved completely. 5 mL n-Butyllithium 2.4 M in hexane and 3.0 mL of dry DMF was added at -78°C. The reaction was warmed up to room temperature and stirring was continued overnight. The resulting mixture was neutralized with 10 mL 3M hydrochloric acid. After extraction with dichloromethane, the organic layer was washed with brine and extracted organic layer was dried with Na₂SO₄ and solvent was removed under reduced pressure give a yellow color of 2,5-dimethoxybenzene-1,4-dicarboxaldehyde compound. Yield: 388mg. Product was characterized by ¹H NMR. ¹H NMR (400 MHz, CDCl₃): δ= 10.50 (s, 2H), 7.46 (s, 2H), 3.95 (s, 6H).

Synthesis of 2,4,6-Tris(4-aminophenyl)-s-triazine (Tz):

In a typical synthesis, 10 mL of chloroform was added to 772 mg (6.5 mmol) of 4-aminobenzonitrile. 2mL of trifluoromethanesulfonic acid was added dropwise at 0 °C under argon protection, and then the system was warmed to room temperature and stir for 24 h. After the reaction was completed, 20 mL of deionized water was added, and the pH was adjusted to neutral with 2 M sodium hydroxide solution, filtered, and the yellow solid was collected and washed with deionized water. Product was characterized by ¹H NMR. ¹H NMR (400 MHz, DMSO-D₆): δ = 8.38 (d, J = 8.7 Hz, 6H), 6.70 (d, J = 8.6 Hz, 6H), 5.96 (s, 6H).

Synthesis of IEP:

2,4,6-Tris(4-aminophenyl)-s-triazine (40 mg, 0.112 mmol) and 2,5-dimethoxyterephthalaldehyde (33 mg, 0.169mmol) were weighed into a Pyrex tube and dissolved in ethanol (3.0 mL), to this o-dichlorobenzene (o-DBC, 3.0mL) was added. Following this, 0.25 mL of aqueous acetic acid (3 M solution) was added to this mixture. Then the Pyrex tube was flash frozen in a liquid nitrogen bath and sealed. The Pyrex tube along with its contents was placed in an oven at 120°C for 3 days. This yielded about 50 mg of yellow coloured solid which was washed with DMF, dioxane, MeOH, Acetone and THF (68%, isolated yield). A soxhlet

extraction/wash was carried out on the final product and the supernatant was analyzed using solution NMR and no peaks corresponding to any organic impurity was found suggesting the sample is free of any dissolved oligomers. Anal. Calcd for $(C_{12}N_2H_9O)_n$: C = 73.08; H = 4.60; N = 14.20. Found: C=73.29; H=4.37; N=14.58.

Synthesis of IEP-MnO₂.

By a simple synthesis method, 5 mg IEP and 10 mg MnO₂ nanocrystals were mixed in 10 mL ethanol, sonicated for 5 min, and then stirred at room temperature for 4 h. The collected dark green product was washed three times with ethanol and vacuum dried at 80 °C for 12 h to obtain IEP-MnO₂.

Synthesis of TPB-DMTP-COF:

A mixture of BuOH/ o-DCB (0.5 mL/0.5 mL), 1,3,5 -Tris(4-aminophenyl)benzene (TPB, 28 mg, 0.08 mmol), 2,5-dimethoxyterephthalaldehyde (Dp, 23.3 mg, 0.12 mmol), and an aqueous acetic acid solution (6 M, 0.1 mL) was degassed in a Pyrex tube (10 mL) by three freeze-pump-thaw cycles. The tube was sealed and heated at 120 °C for 3 days. The precipitate was collected by centrifugation, washed with THF, and dried at 120 °C under vacuum overnight to give TPB-DMTP-COF in 82% yield.

The test conditions of IEP-MnO₂:

IEP-MnO₂ (0.05 mg/mL) was dispersed in DMSO/H₂O PBS buffer (1:9, v/v, 20 mM, pH =7.4) for all titration and selectivity experiments. Unless otherwise noted, the PBS buffer solution used in this research is the same condition and the total volume of detection system is 1 mL.

Characterization:

The Fourier transform infrared spectra (FTIR) were recorded with a Mattson Alpha-Centauri spectrometer (VERTEX 70) in the range 4000–400 cm^{-1} from KBr pellets. Thermogravimetry measurements were performed under N_2 atmosphere with a PerkinElmer TGA-7 thermogravimetric analyzer from 32 $^{\circ}\text{C}$ to 800 $^{\circ}\text{C}$ with a heating rate of 10 $^{\circ}\text{C min}^{-1}$. Specific surface areas and pore volume were calculated by using the Brunauer–Emmett–Teller (BET) method (TriStar3020/ASAP2020M, USA). ^{13}C CP MAS solid-state NMR (SS-NMR) was recorded with a Bruker 150 MHz NMR spectrometer. The UV/Vis spectra for the MnO_2 was collected with a Cary-5000 spectrophotometer. And for the corrected steady-state emission spectra, a Hitachi F-7000 spectrofluorometer was employed. The fluorescence lifetime of IEP, IEP- MnO_2 , IEP- MnO_2 +GSH, IEP- MnO_2 +Cys, IEP- MnO_2 +Hcy were collected by Steady-State & Time-Resolved Fluorescence Spectrofluorometer (FLS920). All pH measurements were finished with a pH-10C digital pH meter. The morphologies of the samples and element mapping spectrum were characterized by transmission electron microscope (TECNAI G² TF20, USA). Powder X-ray diffraction (PXRD) patterns were recorded with a x'pert pro diffractometer at room temperature. The data were collected in the 2θ range from 2.00 to 40.00. The steady-state emission spectra were obtained from F-7000 spectrofluorometer. The presence of Mn^{2+} was determined by iCAPTM Q inductively coupled plasma mass spectrometry (ICP-MS). The structures of the monomers Tz and Dp were characterized by 400 M ^1H NMR spectrum (JNM-ECS). The average size distribution and Zeta potential were measured by Nanoparticle Size and Zeta Potential Analyzer (90Plus Pals) at room temperature using ethanol as the solvent

The limit of detection calculation. The limit of detection (LOD) for GSH and Cys were calculated by the linear function in Figure 4b and 4d and the following equation:

$$\text{LOD} = 3\sigma / k$$

Where σ is the standard derivation of fluorescence intensity of ($I_{523 \text{ nm}}$) IEP-MnO₂ suspension;
 k is the slope of the linear calibration curve in Figure 4b and 4d.

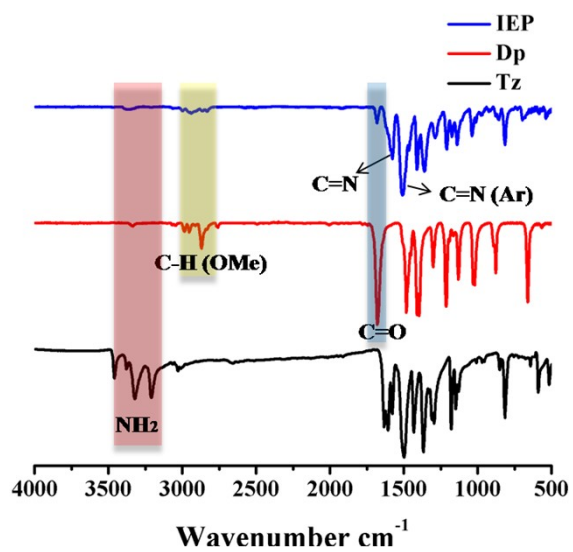


Figure S1. The FT-IR spectrum of IEP, Dp and Tz.

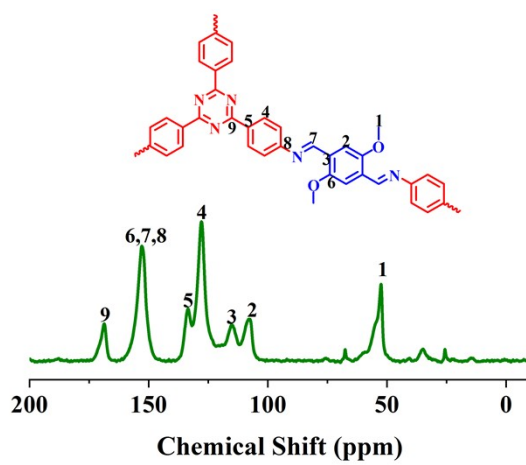


Figure S2. ^{13}C CP/MAS NMR spectra of IEP.

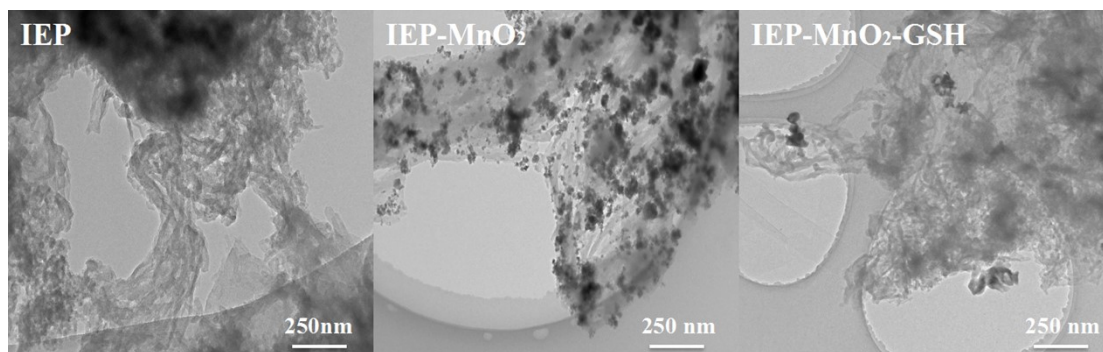


Figure S3. Transmission electron microscope images of IEP, IEP-MnO₂ and IEP-MnO₂+GSH.

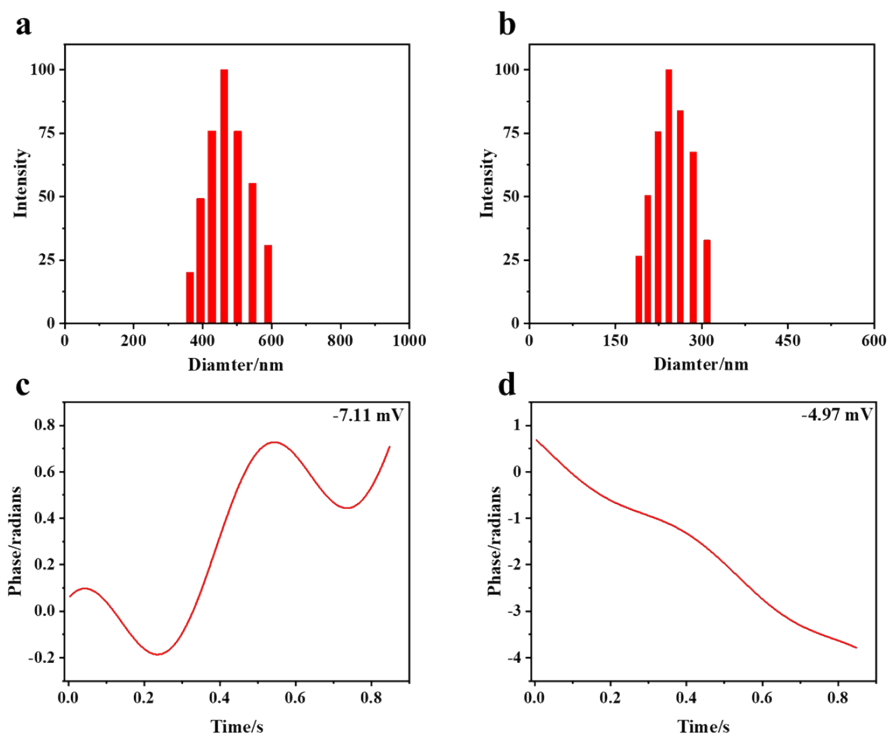


Figure S4. (a, b) Dynamic light scattering (DLS) spectra of IEP and IEP-MnO₂; (c, d) Zeta potential of IEP and IEP-MnO₂.

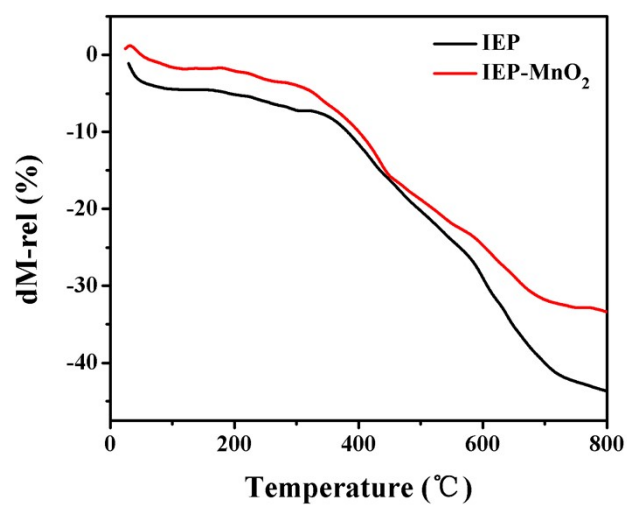


Figure S5. The TGA and of IEP and IEP-MnO₂.

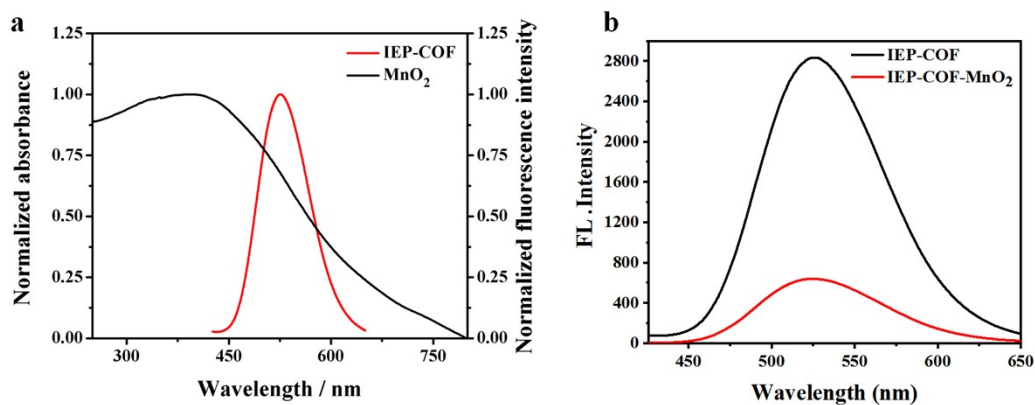


Figure S6. (a) Normalized ultraviolet absorption spectrum of MnO₂ and normalized fluorescence emission spectrum of IEP (the insets are images of IEP and IEP-MnO₂ under the excitation of ultraviolet light at 365 nm); (b) Fluorescence emission spectrum of IEP and IEP-MnO₂ dispersed in PBS buffer solution $C_{\text{IEP}} = C_{\text{IEP-MnO}_2} = 0.05\text{mg/mL}$, $\lambda_{\text{ex}} = 406\text{ nm}$, $\text{pH} = 7.4$.

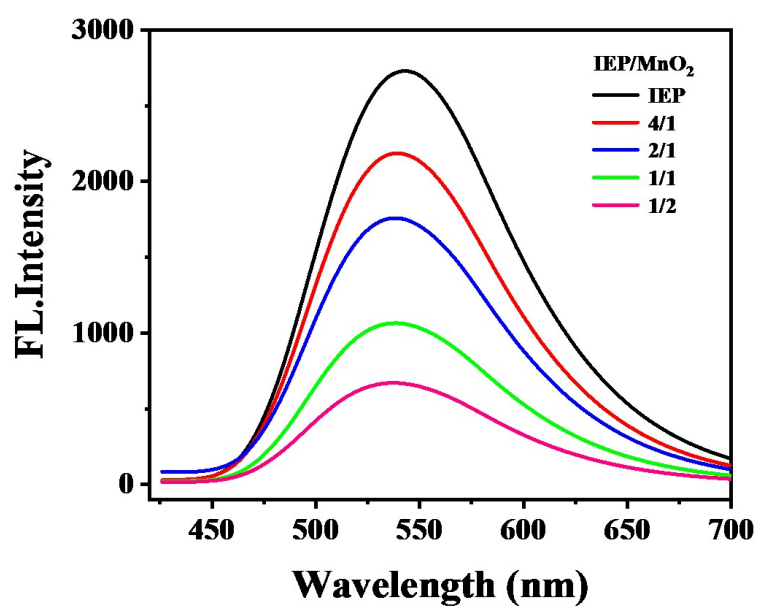


Figure S7. Fluorescence emission spectra of different MnO₂ content IEP-MnO₂ composite materials. $C_{\text{IEP-MnO}_2} = 0.05\text{mg/mL}$, $\lambda_{\text{ex}} = 406\text{ nm}$

Table S1. Comparison between some selected assays for biothiol determination

Materials	GSH		Cys		Refs
	Linear range	Detection limit	Linear range	Detection limit	
CD-I	1–200 μ M	0.3 μ M	5–200	0.3	1
g-C ₃ N ₄ -Ag ⁺	0.02–100 μ M	0.0081 μ M	0.02–100	0.0064	2
PEI-AgNCs	0.5–6 μ M	0.38 μ M	0.1–10	0.042	3
CDs/Hg ²⁺	0.5–10 μ M	0.008 μ M	0.5–10 μ M	0.0076 μ M	4
Mu-Hg ²⁺	0.1–40 μ M	0.01 μ M	0.5–30 μ M	0.02 μ M	5
Hg ²⁺ -Au ⁺	0–0.25 μ M	0.0094 μ M	0–0.25 μ M	0.0083 μ M	6
CdTe QDs-Hg ²⁺	0.6–20 μ M	0.1 μ M	2.0–20 μ M	0.6 μ M	7
N,S-CDs			0.1–11 μ M	0.086 μ M	8
H-CD-Ag ⁺	100–400 μ M	30 μ M	100–600 μ M	30 μ M	9
C-dots/Hg ⁺	0.01–5 μ M	0.0049 μ M	0.01–5 μ M	0.0085 μ M	10
CdTe/CdSe QDs	0.2–100 μ M	0.02 μ M	0.2–100 μ M	0.131 μ M	11
WS ₂	100 pM-10 nM	0.061 nM			12
BP QDs	0.1~5.0 μ M	0.02 μ M	0.1~10.0 μ M	0.03 μ M	13
IEP-MnO ₂	0-1 mM	1.79 μ M	0-2 mM	19.33 μ M	This work

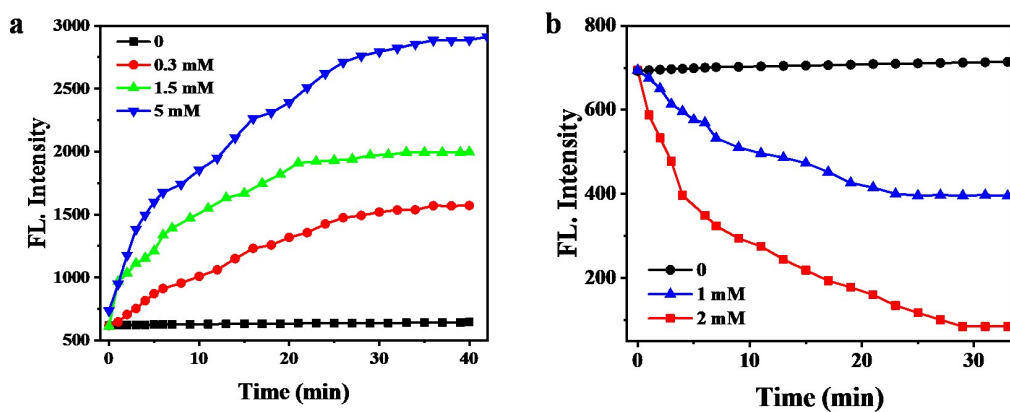


Figure S8. (a) Time-dependent fluorescence spectrums of IEP-MnO₂ with different concentration of GSH (0, 0.3, 1.5, 5 mM); (b) Time-dependent fluorescence spectrums of IEP-MnO₂ with different concentration of Cys (0, 1, 2 mM). $C_{\text{IEP-MnO}_2} = 0.05 \text{ mg/mL}$, $\lambda_{\text{ex}} = 406 \text{ nm}$, $\lambda_{\text{em}} = 523 \text{ nm}$.

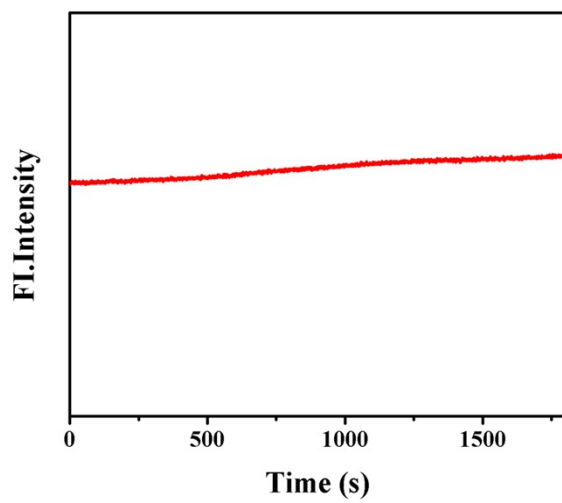


Figure S9. Light stability analysis of IEP-MnO₂.

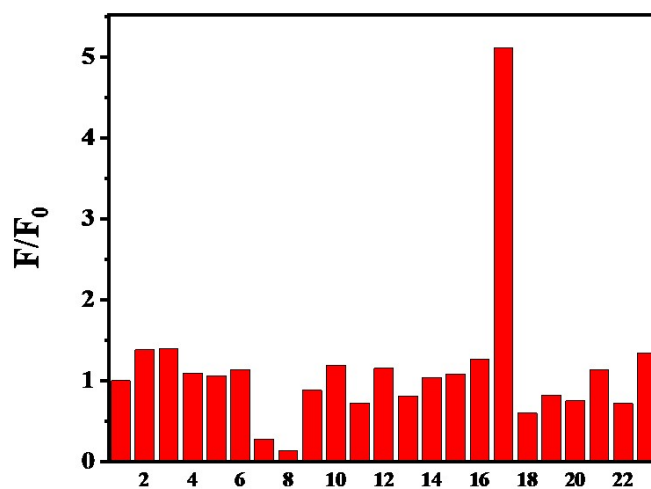


Figure S10. The specific selectivity of IEP-MnO₂ to GSH. (The specie order: IEP-MnO₂, glutamic acid, aspartic acid, glycine, L-hydroxyproline, L-isoleucine, Cys, Homocysteine, L-tyrosine, L-serine, L-lysine, L-Arginine, L-alanine, DL-methionine, DL-tryptophan, L-phenylalanine, GSH, HS⁻, SO₃²⁻, SCN⁻ and SO₄²⁻, H₂O₂, ascorbic acid, the concentration of each species is 5 mM). C_{IEP-MnO₂} = 0.05 mg/mL, λ_{ex} = 406 nm, λ_{em} = 523 nm.

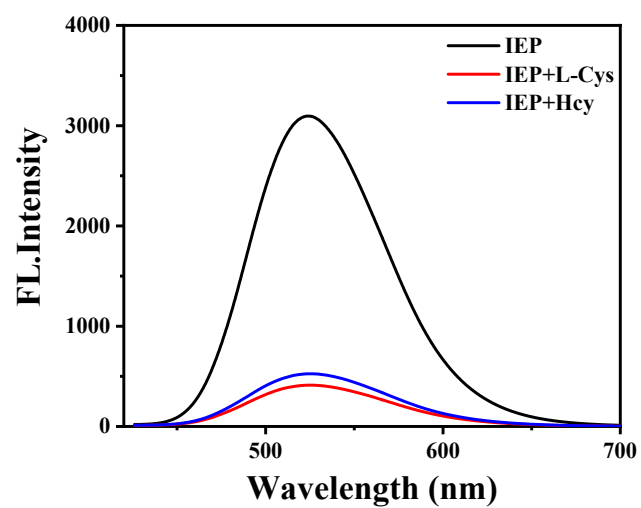


Figure S11. The fluorescence emission spectrum of IEP, IEP+Cys and IEP+Hcy, $\lambda_{\text{ex}}=406$ nm.

$C_{\text{IEP}}=0.05$ mg/mL, $C_{\text{L-Cys}}=C_{\text{Hcy}}=5$ mM.

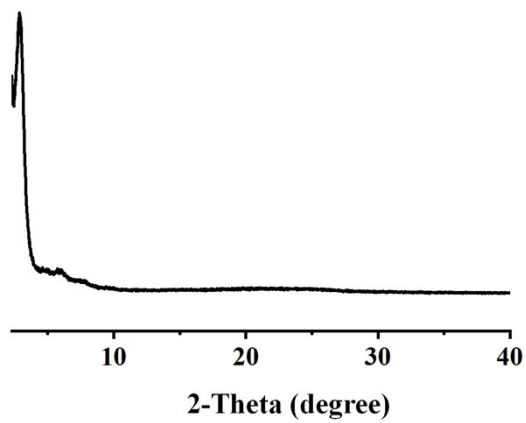


Figure S12. The PXRD pattern of TPB-DMTP-COF.

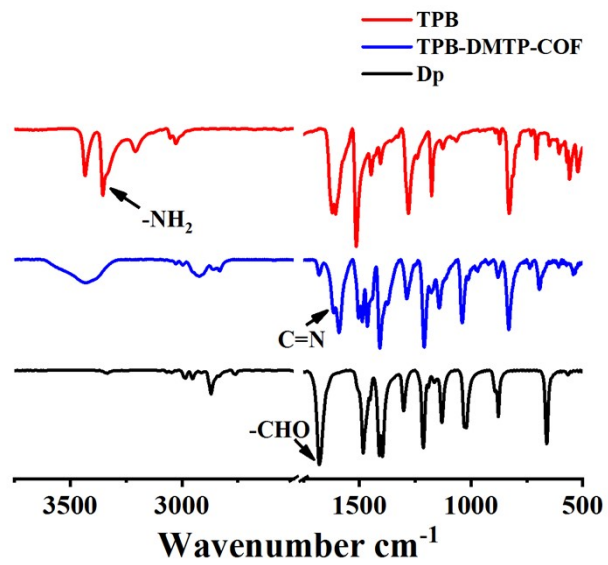


Figure S13. The FT-IR spectrum of TPB, Dp and TPB-DMPT-COF.

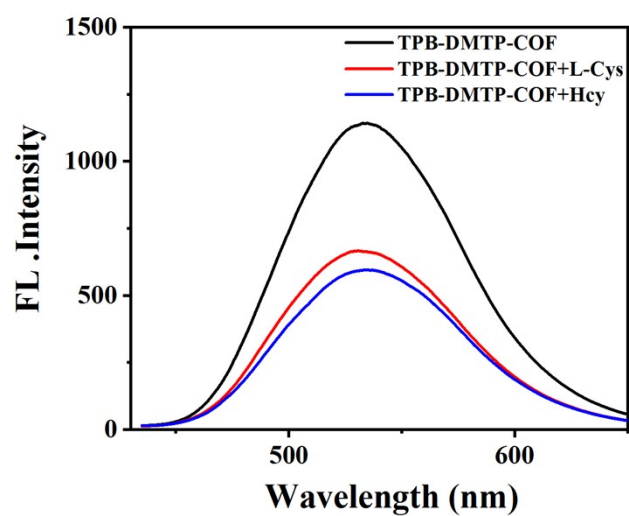


Figure S14. The fluorescence emission spectrum of TPB-DMTP-COF, TPB-DMTP-COF+Cys and TPB-DMTP-COF+Hcy, $C_{\text{TPB-DMTP-COF}} = 0.05 \text{ mg/mL}$, $C_{\text{Cys}} = C_{\text{Hcy}} = 5 \text{ mM}$. $\lambda_{\text{ex}} = 406 \text{ nm}$.

Table S2. The fluorescence lifetimes and percentage of TPB-DMTP-COF, TPB-DMTP-COF + Cys and TPB-DMTP-COF +Hcy (Global analyst results of different emission wavelength at 510 nm, 525 nm and 540 nm). $C_{\text{TPB-DMTP-COF}}=0.05$ mg/mL, $C_{\text{Cys}}=C_{\text{Hcy}}=5$ mM.

Test Group	τ_1 / ns	τ_2 / ns	τ_3 / ns	χ^2
TPB-DMTP-COF	4.15 ± 0.005 (8.44%)	14.96 ± 0.001 (83.98%)	0.68 ± 0.263 (7.58%)	1.060
TPB-DMTP-COF + Cys	3.01 ± 0.006 (13.92%)	14.05 ± 0.001 (65.80%)	0.22 ± 0.1000 (20.28%)	1.152
TPB-DMTP-COF +Hcy	5.52 ± 0.003 (22.53%)	13.24 ± 0.001 (60.73%)	0.27 ± 0.076 (13.74%)	1.052

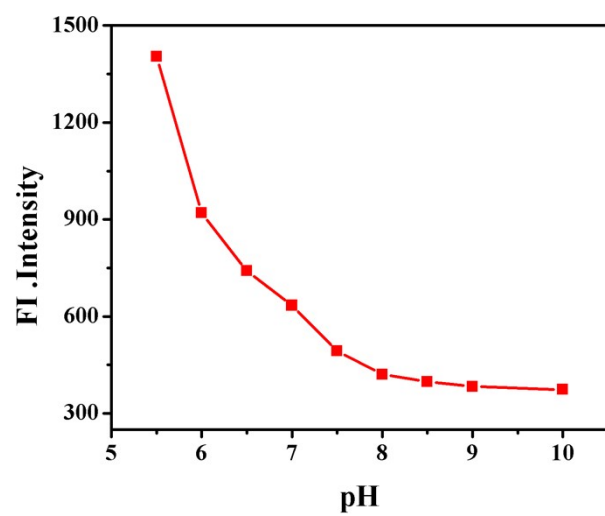


Figure S15. The fluorescence emission intensity of IEP-MnO₂ under different pH conditions.

$\lambda_{\text{ex}}=406 \text{ nm}$, $\lambda_{\text{em}}=523 \text{ nm}$. $C_{\text{IEP-MnO}_2}=0.05 \text{ mg/mL}$.

Table S3. Test results of GSH in human whole blood.

Initial concentration	Add (μM)	Total found (μM)	Recovery (%)	RSD (%) n=3
16.98 μM	20.0	34.9 \pm 2.32	94.29	3.26
	50.0	70.6 \pm 2.65	105.45	2.96
	20.0	39.9 \pm 3.34	108.11	4.02
	50.0	59.8 \pm 2.99	89.27	3.61
	20.0	33.1 \pm 2.48	89.56	3.35
	50.0	60.5 \pm 3.64	90.39	2.75

Table S4. Test results of Cys in human serum.

Initial concentration	Add (μM)	Total found (μM)	Recovery (%)	RSD (%) n=3
6 μM	40.0	44.4 \pm 1.36	96.48	3.56
	90.0	98.4 \pm 3.85	102.53	2.64
	40.0	45.2 \pm 1.32	98.24	4.26
	90.0	100.1 \pm 3.62	104.26	5.34
	40.0	47.0 \pm 1.64	102.17	2.95
	90.0	97.9 \pm 2.34	101.97	3.12

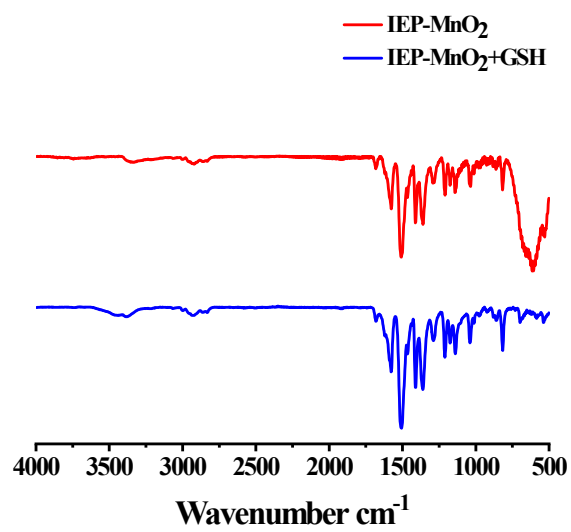


Figure S16. The infrared spectrum of IEP-MnO₂ and IEP-MnO₂+GSH.

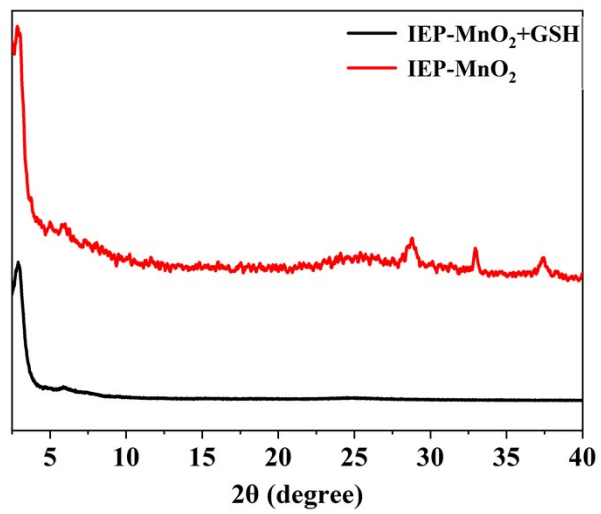


Figure S17. The PXRD pattern of IEP-MnO₂ and IEP-MnO₂+GSH.

References

1. I. Ortiz-Gomez, M. Ortega-Munoz, A. Marin-Sanchez, I. de Orbe-Paya, F. Hernandez-Mateo, L. F. Capitan-Vallvey, F. Santoyo-Gonzalez and A. Salinas-Castillo, *Mikrochim Acta*, 2020, **187**, 421.
2. Y. Tang, H. Song, Y. Su and Y. Lv, *Anal Chem*, 2013, **85**, 11876-11884.
3. N. Zhang, F. Qu, H. Q. Luo and N. B. Li, *Biosens Bioelectron*, 2013, **42**, 214-218.
4. J. Y. Liang, L. Han, S. G. Liu, Y. J. Ju, N. B. Li and H. Q. Luo, *Spectrochim Acta A Mol Biomol Spectrosc*, 2019, **222**, 117260.
5. W. Zhao, M. Sun, T. Lei, X. Liu, Q. Zhang and C. Zong, *Sensors and Actuators B: Chemical*, 2017, **249**, 90-95.
6. K. S. Park, M. I. Kim, M. A. Woo and H. G. Park, *Biosens Bioelectron*, 2013, **45**, 65-69.
7. J. Y. Bingyan Han, and Erkang Wang, *Anal. Chem.*, 2009, **81**.
8. Y. Guo, L. Yang, W. Li, X. Wang, Y. Shang and B. Li, *Microchimica Acta*, 2016, **183**, 1409-1416.
9. Y. Wu, X. Liu, Q. Wu, J. Yi and G. Zhang, *Anal Chem*, 2017, **89**, 7084-7089.
10. L. Zhou, Y. Lin, Z. Huang, J. Ren and X. Qu, *Chem Commun (Camb)*, 2012, **48**, 1147-1149.
11. Y. L. Yi Zhang, and Xiu-Ping Yan, *Anal. Chem.*, 2009, **81**, 5001-5007.
12. L. Li, Q. Wang and Z. Chen, *Mikrochim Acta*, 2019, **186**, 257.
13. L. Ren, H. Li and J. Du, *Mikrochim Acta*, 2020, **187**, 229.